

A Predictive Model for Corrosion Inhibition of Mild Steel by Thiophene and Its Derivatives Using Artificial Neural Network

K.F.Khaled^{1,2*} and N. A. Al-Mobarak³

¹ Electrochemistry Research Laboratory, Ain Shams University, Faculty of Education, Chemistry Department, Roxy, Cairo, Egypt

² Materials and Corrosion Laboratory, Taif University, Faculty of Science, Chemistry Department, Taif, Hawiya 888, Kingdom of Saudi Arabia

³ Chemistry Department, Faculty of Science, Princess Nora Bint Abdulrahman University, Riyadh, Saudi Arabia

*E-mail: khaledrice2003@yahoo.com

Received: 5 August 2011 / Accepted: 3 January 2012 / Published: 1 February 2012

Corrosion inhibition performance of thiophene and its derivatives were studied using potentiodynamic polarization. The study used the artificial neural network analysis effectively generalized correct responses that broadly resemble the data in the training set. The neural network can now be put to use with the actual data, this involves feeding the neural network values for Hammett constants, dipole moment, HOMO energy, LUMO energy and energy gap. The analysis produced instantaneous results of corrosion inhibitor efficiency. The predictions were reliable, provided the input values are within the range used in the training set.

Keywords: Mild steel; Modeling studies; Polarization; Acid inhibition

1. INTRODUCTION

Owing to the increasing ecological awareness, as well as the strict environmental regulations, and consequently the need to develop environmentally friendly processes, attention is currently focused on the development of “green” alternatives to mitigating corrosion. Green approaches to corrosion mitigation entail the use of substances, techniques, and methodologies that reduce or eliminate the use of generation of feedstocks, products, by-products, solvents, reagents, and so forth that are hazardous to human health or the environment in combating corrosion.

Thiophene based compounds have been a constant matter of investigation due to their wide range of applications. They are the precursors of many drugs with high therapeutical potential, being

used in the treatment of cancer [1–3], osteoporosis [4], hypertension [5], Alzheimer's disease [6], human immunodeficiency virus (HIV-1) [7–9], and others.

Heterocyclic compounds represent a potential class of corrosion inhibitors. There is a wide range of studies regarding corrosion inhibition by nitrogen-containing heterocyclic compounds [10–17]. Heterocyclic compounds containing both nitrogen and sulfur atoms are of particular importance as they often provide excellent inhibition compared with compounds containing only nitrogen or sulfur [18–24]. The corrosion-inhibiting property of these compounds is attributable to their molecular structure.

Being used in chemistry during the second half of 20th century as an extended statistical analysis [25–32], the quantitative structure-activity relationship (QSAR) method had attained in recent years a special status, officially certified by European Union as the main computational tool (within the so called “*in silico*” approach) for the regulatory assessments of chemicals by means of non-testing methods [33–38].

Actually, the chemical-physical advantage of QSAR stands in its multi-linearity correlation that resembles with superposition principle of quantum mechanics, which allow meaningful interpretation of the structural (inherently quantum) causes associated with the latent or unobserved variables (sometimes called as *common factors*) into the observed effects (activity) usually measured in terms of 50%-effect concentration (EC50) [39,40].

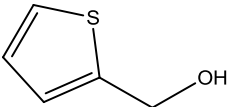
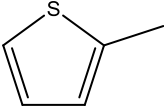
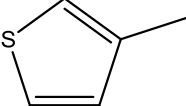
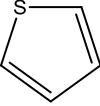
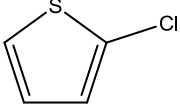
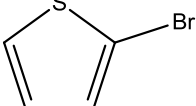
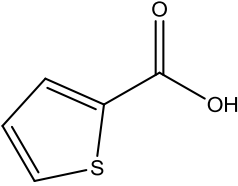
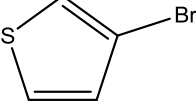
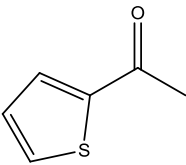
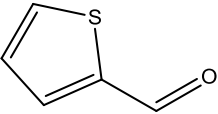
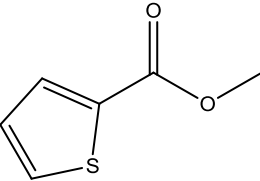
Although undoubtedly useful, the “official” trend in employing QSAR methods is to classify, over-classify and validate through (external or molecular test set) prediction, a gap between the molecular computed orderings and the associate mechanistic role in corrosion inhibition assessment remains as large as the QSAR strategy has not turned into a versatile tool in identifying the structural properties and its role in corrosion inhibition process by means of structurally selected common variables; that is to use QSAR information for internal mechanistic predictions among training molecules to see their inter-relation respecting the whole class of observed efficiencies employed for a specific correlation.

The present work aims to start filling this gap by deepening the modeling of structural properties of the inhibitor molecules and their inhibition efficiencies through extending the main concepts of recent developed in QSAR, developed the fully algebraic version of traditional statistically optimized QSAR picture, targeting the quantification of the competition between molecular structure properties and their inhibition efficiencies. Also, the aim of this study is to present a predictive model for corrosion inhibition of mild steel by thiophene and its derivatives using artificial neural network. The proposed model obtains predictions of inhibition efficiencies based on several quantum chemical variables and comparing these predicted values with the experimental inhibition efficiencies.

2. EXPERIMENTAL DETAILS

The structures of the thiophene and its derivatives are presented in Table 1. All the investigated compounds were obtained from Aldrich chemical co., they were put in 0.5 M H₂SO₄ (Fisher Scientific) without pre-treatment at concentrations of 0.01M.

Table 1. Molecular structures of thiophene and ten of its derivatives.

#	Inhibitor name	Structure
1	2-hydroxymethylthiophene	
2	2-methylthiophene	
3	3-methylthiophene	
4	Thiophene	
5	2-chlorothiophene	
6	2-bromothiophene	
7	2-thiophenecarboxylic acid	
8	3-bromothiophene	
9	2-acetylthiophene	
10	2-thiophenecarboxaldehyd	
11	2-thiophenecarboxylic acid methyl ester	

All dc electrochemical measurements were performed in a typical three-compartment glass cell consisted of the mild steel rod (C = 0.10 wt.% , Cu= 0.1 wt.% Cr=0.12 wt.%, Si=0.05 wt.%, Mn= 0.9 wt.% , Fe = Balance) its surface area 0.28 cm^2 as working electrode (WE) (prepared using emery papers of different grit sizes up to 4/0 grit, polished with Al_2O_3 ($0.5 \mu\text{m}$ particle size), platinum mesh as counter electrode (CE), and a saturated calomel electrode (SCE) as the reference electrode. Solutions were prepared from bidistilled water. The electrode potential was allowed to stabilize for 60 min before starting the measurements. All experiments were conducted at 25°C . The electrolyte solution was made from analytical reagent grad H_2SO_4 .

The electrodes were arranged in such a way that one-dimensional potential field existed over the WE surface in solution. To get an impression about the process occurred at the mild steel/acid interface, Tafel curves were obtained by changing the electrode potential automatically from $(-750 \text{ to } -280 \text{ mV}_{\text{SCE}})$ versus open circuit potential with scan rate of 5 mV/s . Measurements were performed with a Gamry Instrument Potentiostat/Galvanostat/ZRA. This includes a Gamry Framework system based on the ESA400, Gamry applications that include DC105 for dc corrosion measurements, Echem Analyst 5.58 Software was used for plotting, graphing and fitting data.

3. COMPUTATIONAL METHOD

Geometrical parameters of all stationary points for the investigated thiophene and its derivatives are optimised by employing analytic energy gradients. The generalised gradient approximation (GGA) within the density functional theory was conducted with the software package DMol³ in Materials Studio of Accelrys Inc [41]. All calculations were performed using the Becke–Lee–Yang–Parr (BLYP) exchange correlation functional and the double numerical with polarization (DNP) basis set [42–44], since this was the best set available in DMol³. A Fermi smearing of 0.005 hartree and a real space cutoff of 3.7 \AA was chosen to improve the computational performance. All computations were performed with spin polarization.

The phenomenon of electrochemical corrosion takes place in the liquid phase, so it is relevant to include the effect of solvent in the computations. Self-Consistent Reaction Field (SCRf) theory [45], with Tomasi's polarised continuum model (PCM) was used to perform the calculations in solution. These methods model the solvent as a continuum of uniform dielectric constant ($\epsilon=78.5$) and define the cavity where the solute is placed as a uniform series of interlocking atomic spheres. Frontier orbital distribution was obtained, at the same basis set level, to analyse the reactivity of inhibitor molecules.

3.1. Artificial Neural Networks

Neural network analysis is an artificial intelligence (AI) approach to mathematical modeling. It is a sophisticated model-building technique capable of modeling data may be better represented by non-linear functions. Corrosion phenomena is a complex , non- linear that are too complex to be

described by analytical methods or empirical rules which make it an ideal phenomena to be studied using artificial neural networks.

Neural networks are inspired by the way the human brain works. The brain consists of billions of neurons, which are linked together into a complex network. A neuron communicates with another by sending an electrical signal along an axon, which is a long nerve fibre that connects to the second neuron at a synapse. Each neuron acts an information processing element because the electrical signals sent out by one neuron depend on the strength of the incoming signals at its synapses.

3.2. The structure of a neural network

The structure of the artificial neural network is presented in Fig. 1.

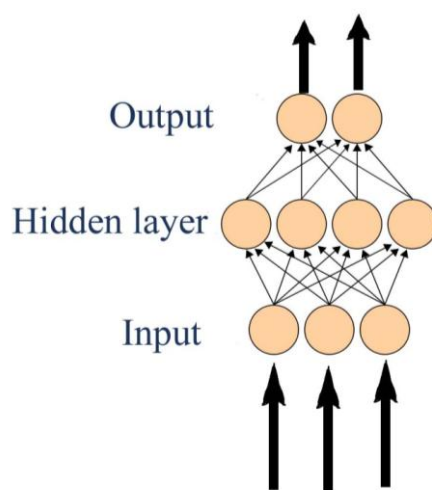


Figure 1. Structure of artificial neural network

The lower layer represents the input layer. The input layer is used to introduce the input (predictor) variables to the network. The upper layer is the output layer. The outputs of the nodes in this layer represent the predictions made by the network for the response variables. This network also contains a **single hidden layer with four nodes**. Each node (other than those in the input layer) takes as its input a transformed linear combination of the outputs from the nodes in the layer below it. This input is then passed through a transfer function to calculate the output of the node. The **transfer** function used by QSAR is an s-shaped **sigmoid function**. This function is chosen because it is smooth and easily differentiable, features that help the algorithm that is used to train the network [46].

3.3. Training process and topology of the neural network

Training is the process whereby the connection weights and biases are set so as to minimize the prediction error for the network. For a particular set of weights and biases, each of the training cases

are introduced to the network and an error function is used to determine how well the calculated outputs match the expected output values.

It has been found empirically that a single hidden layer is sufficient for modeling most data sets and it is recommended that we first try to model our data with a single hidden layer. Additional hidden layers allow the neural network to model more complex functions. There is a formal proof, the Kolmogorov theorem which states that two hidden layers are theoretically sufficient to model any problem, though it is possible that, for some data sets, a network with more hidden layers might be able to find a good model more easily [46].

Each connection weight and node bias is a parameter that can be adjusted during network training. Hence, each connection and node corresponds to one degree of freedom of the model represented by the neural network. As a general rule, we should aim to have at least twice as many observations as there are degrees of freedom. If we have too many nodes in the hidden layer(s), then the model will tend to overfit our data. If we have too few, then the model may not have sufficient power to fit our data.

4. RESULTS AND DISCUSSION

4.1. Inhibition study

Evaluation of the inhibition efficiencies can be performed through electrochemical experiments which consist of the determination of current density/potential curves. Figure 2 shows the dc polarization curves of mild steel in 0.5 M sulfuric acid without and with thiophene and its derivatives in concentration of 0.01M at 25 °C. The extrapolation of the Tafel straight line allows the potential (E_{corr}), cathodic, anodic Tafel slopes and inhibition efficiency ($\Pi\%$) as a function of thiophene and its derivatives are given in Table 2. The inhibition efficiency ($\Pi\%$) is given in equation 1

$$\Pi\% = \left(1 - \frac{i_{\text{corr}}}{i_{\text{corr}}^o}\right) \times 100 \quad (1)$$

where i_{corr}^o and i_{corr} are corrosion current densities in absence and presence of thiophene and its derivatives.

From Fig. 2, it does not appear definite shift of the corrosion potential (E_{corr}) which depends on inhibitor type. At the examined inhibitors concentration a cathodic plateau seems to be formed. Thiophene and its derivatives exerted inhibitive action both on anodic dissolution of metal and on the cathodic oxygen reduction reaction. In each case the whole curves shifted towards lower corrosion current density values compared to that of the blank solution. In anodic domain, it is noted in the presence of thiophene and its derivatives, a change in Tafel anodic coefficient compared to mild steel without inhibitors. This effect is attributed to the modification of the reactional process due to the formation of a protective film on the electrode surface rather than a simple adsorption on the active sites. This would result in a reduction of the current densities. In the cathodic domain, a diffusional

mechanism was observed characterized by a plateau which does not change when thiophene and its derivatives molecules are added to the corrosive medium. This suggests that thiophene and its derivatives do not modify the mechanism or the nature of the electrochemical reaction involved.

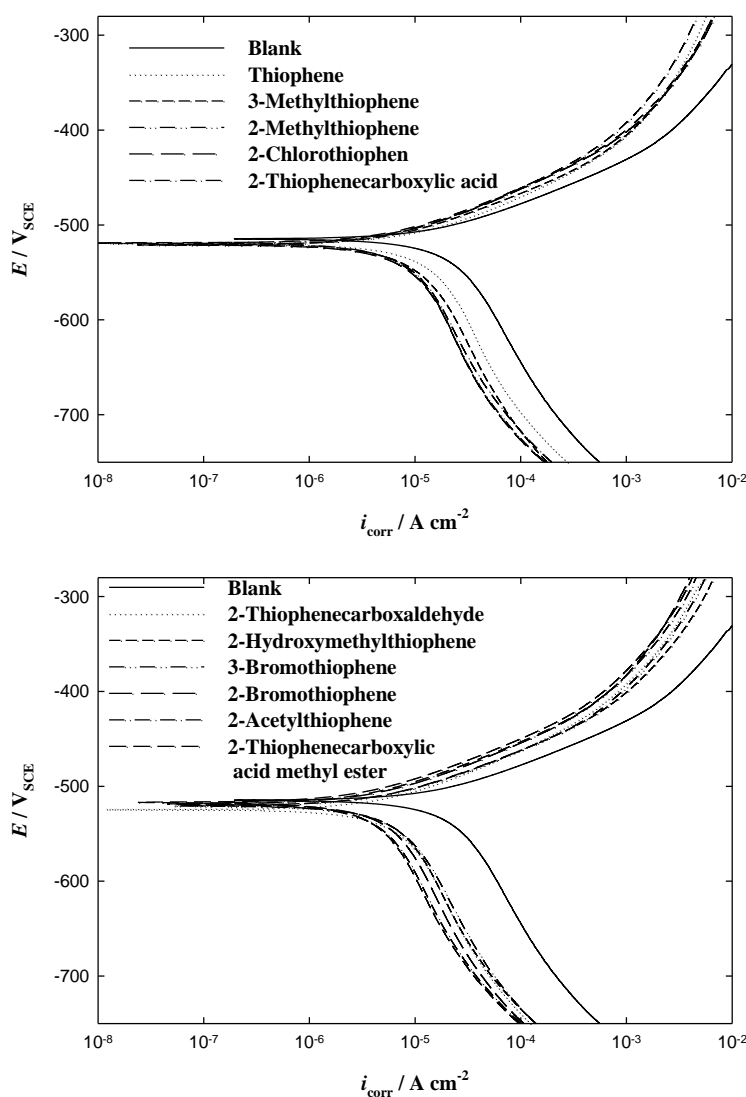


Figure 2. Cathodic and anodic polarization curves recorded for the mild steel electrode in aerated stagnant 0.5 M H₂SO₄ solutions, at a scan rate of 5 mV s⁻¹ at 25°C±1, without and with various thiophene and its derivatives

The analysis of the results obtained in Table 2 shows that the reduction of the corrosion current density and consequently an increase of inhibition efficiencies depend on the structure of the studied derivatives. The reduction of anodic and cathodic currents by adding thiophene derivatives can be explained by the blocking of active sites with the formation of a protective film on the mild steel surface.

Table 2. Electrochemical polarization parameters for mild steel in absence and presence of 0.01 M of thiophene and ten of its derivatives in 0.5 M sulfuric acid at 25°C±1.

	$i_{\text{corr}}/\mu\text{A cm}^{-2}$	$-E_{\text{corr}}/\text{mV}$	$\beta_a / \text{mV dec}^{-1}$	$\beta_c / \text{mV dec}^{-1}$	C.R./mpy	$\Pi\%$
0.5 M H ₂ SO ₄	20.52	514.6	49.4	187.1	33.5	---
2-hydroxymethylthiophene	6.47	520.3	48.5	208	2.95	68.4
2-methylthiophene	8.159	518.9	52.8	214.3	3.73	60.2
3-methylthiophene	9.13	520.9	51.9	193.7	4.2	55.5
thiophene	13.22	519.4	55.18	217.3	6.1	35.5
2-chlorothiophene	8.116	520.8	53.12	209.7	3.71	60.4
2-bromothiophene	5.439	518.3	50.4	211.3	2.48	73.5
2-thiophenecarboxylic acid	7.771	519.3	52.12	192.2	3.55	62.1
3-bromothiophene	6.366	520.6	49.0	192.0	2.91	68.9
2-acetylthiophene	4.444	518.7	48.35	205.5	2.03	78.3
2-thiophenecarboxaldehyd	6.743	523.9	53.56	211.8	3.08	67.1
2-thiophenecarboxylic acid methyl ester	4.157	516.8	48.44	208.2	1.9	79.7

Table 3. (Study Table). Descriptors for thiophene and its derivatives calculated using quantum chemical methods

Inhibitor number	Experimental Inhibition Efficiencies	Hammett Constant	Total Dipole Moment (e Å)	HOMO (eV)	LUMO (eV)	Energy gap (LUMO-HOMO), eV	Surface Area (Å ²)	Molecular Volume (Å ³)	Neural Network Prediction for Experimental Inhibition Efficiencies
1	68.4	-0.200 ^(a)	1.861	-8.747	-0.4148	8.3322	138.161	106.289	66.39
2	60.2	-0.170	0.453	-8.497	-0.1543	8.3427	128.185	97.2008	62.38
3	55.5	-0.069	0.812	-8.55	-0.167	8.3830	128.348	97.4409	58.94
4	35.5	0.000	0.376	-8.709	-0.1924	8.5166	105.265	80.0180	43.57
5	60.4	0.226	1.428	-8.809	-0.5235	8.2855	120.939	93.7375	59.26
6	73.5	0.232	1.370	-8.8307	-0.5859	8.2448	125.685	98.0379	69.22
7	62.1	0.265	4.073	-9.3557	-1.439	7.9167	145.912	111.034	78.28
8	68.9	0.395	1.082	-0.922	-0.5507	0.3713	126.392	98.1291	68.32
9	78.3	0.516	4.450	-9.1452	-1.2978	7.8474	154.133	118.573	76.703
10	67.1	0.570 ^(a)	4.587	-9.1906	-1.412	7.7784	132.910	101.803	69.23
11	79.7	0.630 ^(a)	3.135	-9.298	-1.3407	7.9573	166.886	128.453	79.7

Many workers have attempted to establish a quantitative correlation between the electronic configuration, particularly the charge distribution within the molecule, and the inhibitor efficiency of the given organic compound. Special consideration was devoted to the electron density on the atom or group responsible for adsorption [47].

Thiophene, with pyrrole and furan, belong to heterocyclic five-membered aromatic compounds. In this group the position of thiophene is peculiar, since its aromatic character is much closer to benzene than that of the other two compounds [48]. Another reason for the choice of thiophene follows

from its comparatively high adsorptivity due to the presence in its molecule of the sulphur atom with two pairs of free electrons able to form coordinate bonds [47].

To establish a quantitative structure and activity relationship, QSAR, we have changed the electron density in defined position caused by introduction of substituents to the thiophene molecule. For nucleophilic substituents such as 2-CH₂OH, 2-CH₃, or 3-CH₃, which increase the electron density in the aromatic ring, the Hammett constants are negative (Table 3). For electrophilic substituents such as 2-COCH₃, 2-CHO, or 2-COOCH₃, which withdraw electrons from the thiophene ring, the Hammett constants are positive. The values of the Hammett constants [47] calculated by Hammett [49] and Jaffe [50]. Data marked (a) were calculated from the shift of the NMR spectrum for hydrogen atoms in positions 2, 3 and 4 in the thiophene [51]. Several structural parameters have been calculated and presented in Table 3.

4.2. QSAR study using artificial neural network

In this work, a neural network training set was used to predict the corrosion inhibition efficiencies for thiophene and ten of its derivatives used to inhibit the corrosion of mild steel in 0.5 M sulphuric acid solutions.

Table 4. Univariate analysis of the experimental inhibition efficiencies data

B : Experimental Inhibition Efficiencies	
Number of sample points	11
Range	44.2
Maximum	79.7
Minimum	35.5
Mean	64.51
Median	67.1
Variance	136.98
Standard deviation	12.27
Mean absolute deviation	8.88
Skewness	-0.898
Kurtosis	0.251

A study table presented in Table 3 contains the calculated descriptors and properties for the studied thiophene and its derivatives for developing quantitative structure activity relationships and property prediction.

Before searching for potential QSAR, it is worth assessing the quality and distribution of data in the study table (Table 3). Most forms of multivariate analysis assume that the input variables have a normal distribution, and are a representative sample. To examine data in Table 3, a univariate analysis which is a technique used for generating statistics independently for the experimental inhibition

efficiencies. Table 4 shows accepted normal distribution which enables us to start building a correlation matrix. The normal distribution behavior of the studied data was confirmed by the values of standard deviation, mean absolute deviation, variance, skewness and kurtosis, description of these parameters have been reported elsewhere [52].

Table 5. Correlation matrix of the studied variables

	Experimental Inhibition Efficiencies	Hammett Constant	Total Dipole Moment (e Å)	HOMO (eV)	LUMO (eV)	Energy gap (LUMO- HOMO), eV	Surface Area (Å ²)	Molecular Volume (Å ³)
Experimental Inhibition Efficiencies	1	0.5793	0.5516	0.0549	-0.5832	-0.1870	0.78214	0.81727
Hammett Constant	0.5793	1	0.7099	0.0966	-0.8283	-0.2848	0.53425	0.56117
Total Dipole Moment (e Å)	0.5516	0.7099	1	-0.324	-0.9560	0.11902	0.69946	0.69617
HOMO (eV)	0.0549	0.0966	-0.324	1	0.23198	-0.9759	-0.2297	-0.2021
LUMO (eV)	-0.583	-0.828	-0.956	0.2319	1	-0.0145	-0.7316	-0.7348
Energy gap (LUMO-HOMO), eV	-0.187	-0.2848	0.1190	-0.9759	-0.0145	1	0.07236	0.04323
Surface Area (Å ²)	0.7821	0.5342	0.6994	-0.2297	-0.7316	0.0723	1	0.99736
Molecular Volume (Å ³)	0.8172	0.5612	0.6962	-0.2021	-0.7348	0.0432	0.99736	1

Table 5 shows a correlation matrix which is a table of all possible pairwise correlation coefficients for a set of variables. It can be help to identify highly correlated pairs of variables, and thus identify redundancy in the data set.

Each cell of the matrix corresponds to the correlation between two columns of study table data. The correlation coefficients lie between -1.0 and +1.0. A value approaching +1.0 indicates that the two columns are highly correlated and a value approaching -1.0 also indicates a high degree of correlation, except that the data changes values in opposite directions. A correlation coefficient close to 0.0 indicates very little correlation between the two columns. The diagonal of the matrix always has the value 1.0. To aid in visualizing the results, the cells in the correlation matrix grid are colored according to the correlation value in each cell. A standard color scheme is used when the correlation matrix is generated: $+0.9 \leq X \leq +1.0$ (orange), $+0.7 \leq X < +0.9$ (yellow), $-0.7 < x < +0.7$ (white), $-0.9 < x < -0.7$ (yellow) and $-1.0 \leq x \leq -0.9$ (orange).

After constructing the correlation matrix in Table 5 , now it is ready to perform a regression analysis of the descriptor variables compared against the measured corrosion inhibition values. There are two separate issues to consider. First, there are many more descriptor variables than measured

inhibition values, so we should reduce the number of descriptors. Typically, a ratio between two and five measured values for every descriptor should be sought in order to prevent overfitting. Secondly, we are aiming to obtain a parametric representation of the regression, producing a simple equation which can be validated against our scientific knowledge[46].

The cross validation data for the neural network model operates by repeating the calculation several times using subset of the original data to obtain a prediction model and then comparing the predicted values with the actual values for the omitted data. The key measure of the predictive power of the model is the correlation coefficient r^2 . The closer the value is to 1.0 the better the predictive power. For a good model r^2 value should be fairly close to 1.0. the correlation coefficient r^2 for this study is equal to 0.958 which is reasonably high that indicates the predictive power of the model.

Investigation of the neural network analysis in QSAR study shows that the network has too many degrees of freedom (usually the number of network connections between nodes) for the number of observations (rows of data) for which the network is being trained. In this study there is **one hidden layer with three nodes.**

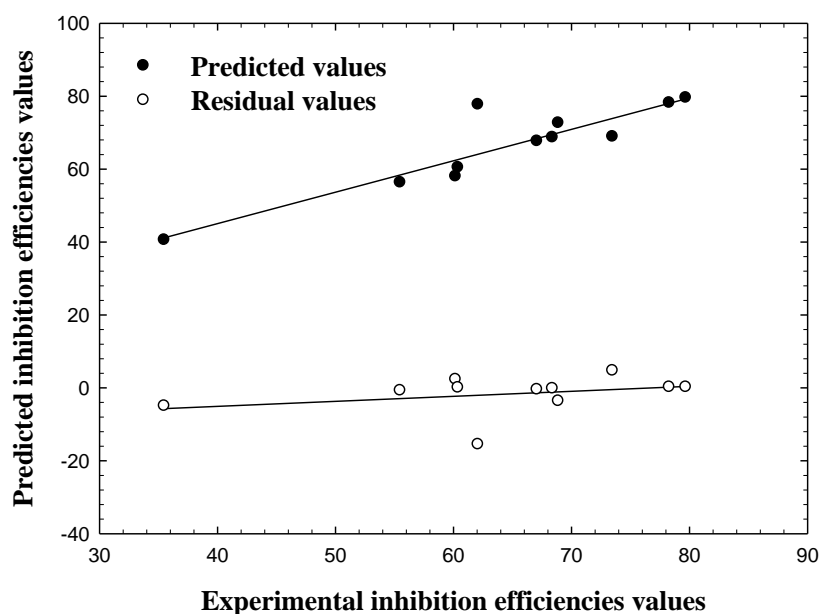


Figure 3. Plot of predicted inhibition and residuals versus measured corrosion inhibition

Applying the neural network prediction model, generates a model containing predictions corresponding to each output of the neural network. The neural network model adds a new column containing a calculation of the model to the study table (Table 3). Also, residual values of the predictions corresponding to each output of the neural network.

Figure 3 shows a relation between the predicted values, residual values and the experimental data in Table 3. A residual can be defined as the difference between the predicted value in the generated model and the measured value for corrosion inhibition. To test the constructed QSAR model, potential outliers have been identified in Fig. 4. An outlier can be defined as a data point whose

residual value is not within cross validated r^2 values, is also, high, even though the regression is significant according to F-test.

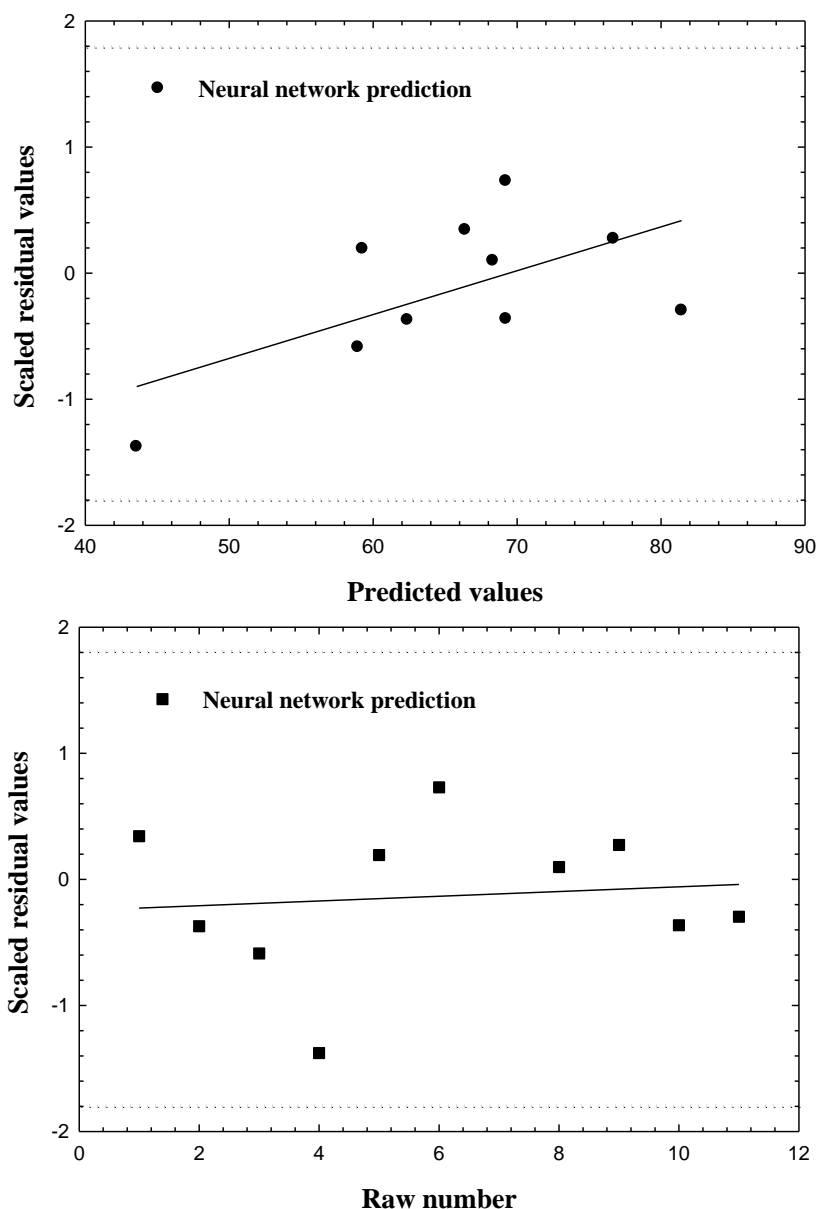


Figure 4. Outlier analysis for inhibition efficiency

Fig. 4 contains two charts. One contains the residual values plotted against the corrosion inhibition measurements and the other displays the residual values plotted against Table 3 raw number. Each chart contains a dotted line that indicates the critical threshold of two standard deviations beyond which a value may be considered to an outlier. Inspection of Fig. 4 shows that there is no points appeared outside the dotted lines which make the QSAR model acceptable.

5. CONCLUSIONS

In spite of the huge success that has been attributed to the use of computational chemistry in corrosion studies, most of the ongoing researches on the inhibitory potentials of organic inhibitors are restricted to laboratory work. DC polarization method used to ascertain the instantaneous inhibition efficiency of the thiophene derivatives. QSAR approach is still an effective method that can be used together with the experimental techniques to predict inhibitor candidates for corrosion process. The study has demonstrated that the neural network can effectively generalize correct responses that only broadly resemble the data in the training set. The neural network can now be put to use with the actual data, this involves feeding the neural network the values for Hammett constants, dipole moment, HOMO energy, LUMO energy, energy gap, molecular area and volume. The neural network will produce almost instantaneous results of corrosion inhibitor efficiency. The predictions should be reliable, provided the input values are within the range used in the training set.

ACKNOWLEDGMENT

Author is grateful for the financial support provided by Taif University project # 1-432-1128 titled "Understanding corrosion inhibition: Study of thiophene compounds on steel surfaces" and the centre of research excellence in corrosion located at King Fahd University, Project # CR-03-2010 titled "Designing new corrosion inhibitors by QSAR and Molecular Dynamics Approaches.

References

1. W. N. Neira, M. I. Rivera, G. Kohlhagen, M. L. Hursey, P. Pourquier, E. A. Sausville and Y. Pommier, *Mol. Pharmacol.*, 56 (1999) 478.
2. R. Villar, I. Encio, M. Migliaccio, M. J. Gil and V. Martinez-Merino, *Bioorg. Med. Chem.*, 12 (2004) 963-968.
3. M. B. Sahasrabudhe, M. K. Nerurkar, M. V. Nerurkar, B. D. Tilak and M. D. Bhavsar, *Br. J. Cancer*, 14 (1960) 547-554.
4. A.V. Kalinin, M. A. Reed, B. H. Norman and V. Snieckus, *J. Org. Chem.*, 68 (2003) 5992-5999.
5. R. K Russell, J. B. Press, R. A. Rampulla, J. J. McNally, R. Falotico, J. A. Keiser, D. A. Bright and A. Tobia, *J. Med. Chem.*, 31 (1988) 1786-1793.
6. W. C. McCormick and I. B. Abrass, *Lancet* 352 Supl. IV (1998) 6.
7. C. E. Stephens, T. M. Felder, J. W. Sowell, G. Andrei, J. Balzarini, R. Snoeck and E. De Clercq, *Bioorg. Med. Chem.*, 9 (2001) 1123-1132.
8. J. B. Hudson, R. J. Marles, C. S. Breau, L. Harris and J. T. Arnason, *Photochem. Photobiol.*, 60 (1994) 591-593.
9. G. Guillet, J. Harmatha, T. G. Waddell, B. J. R. Philog_ne and J. T. Arnason, *Photochem. Photobiol.*, 71 (2000) 111-115.
10. S.L. Granese, B.M. Rosales, C. Oviedo and J.O. Zerbino, *Corros Sci.* 33 (1992) 1439-1453.
11. G. Subramaniam, K. Balasuramaniam and P. Shridhar, *Corros. Sci.* 30 (1990) 1019.
12. S.N. Banerjee and S. Mishra, *Corrosion* 45 (1989) 780-783.
13. S. Hettiarachchi, Y.W. Chain, R.B. Wilson Jr and V.S. Agarwala, *Corrosion* 45 (1989) 30.
14. C.R. Anderson and G.M. Schmid, *Corros. Sci.* 24 (1984) 825-830.
15. E. Stupnisek-Lisac, M. Meticos-Hukovic, D. Lencic, J. Vorkapic-Furac and K. Berkovic, *Corrosion* 48 (1992) 924.
16. E. Stupnisek-Lisac, K. Berkovic and J. Vorkapic-Furac, *Corros. Sci.* 12 (1988) 1189-1202.

17. S.N. Raicheva, B.V. Aleksiev and E.J. Sokolov, *Corros. Sci.* 34 (1993) 343-350.
18. M. Ajmal, A.S. Mideen and M.A. Quraishi, *Corros. Sci.* 36 (1994) 79-84.
19. M.A. Quraishi, M.A.W. Khan, M. Ajmal and S. Muralidharan, *Portg Electrochem. Acta.* 13 (1995) 63-78.
20. M.A. Quraishi, M.A.W. Khan, M. Ajmal, S. Muralidharan and S.V. Iyer, *AntiCorros. Meth. Mater.* 43 (1996) 5-8.
21. M.A. Quraishi, M.A.W. Khan, M. Ajmal, S. Muralidharan and S.V. Iyer, *J. Appl Electrochem.* 26 (1996) 1253-1258.
22. M.A. Quraishi, M.A.W. Khan, M. Ajmal, S. Muralidharan and S.V. Iyer, *Br. Corros. J.* 32 (1997) 72-76.
23. M.A. Quraishi, M.A.W. Khan, M. Ajmal, S. Muralidharan and S.V. Iyer, *Corrosion* 53 (1997) 475.
24. ASTM (American Society for Testing and Materials), 'Metal Corrosion, Erosion and Wear, (Annual Book of ASTM standards 1987) 0.3.02,G1-72.
25. T. W. Anderson *An Introduction to Multivariate Statistical Methods*; Wiley: New York, USA, 1958.
26. N. R. Draper, H. Smith, *Applied Regression Analysis*, Wiley: New York, USA, 1966.
27. J. Shorter, *Correlation Analysis in Organic Chemistry: An Introduction to Linear Free Energy Relationships*; Oxford Univ. Press: London, UK, 1973.
28. G. E. P. Box, W. G. Hunter, J.S. Hunter, *Statistics for Experimenters*; John-Wiley: New York, USA, 1978.
29. J. R. Green, D. Margerison, *Statistical Treatment of Experimental Data*; Elsevier: New York, USA, 1978.
30. J. Topliss, *Quantitative Structure-Activity Relationships of Drugs*; Academic Press: New York, USA, 1983.
31. J. K. Seyfel, *QSAR and Strategies in the Design of Bioactive Compounds*; VCH Weinheim: New York, USA, 1985.
32. S. Chatterjee, A. S. Hadi, B. Price, *Regression Analysis by Examples*, 3rd Ed.; John-Wiley: New-York, USA, 2000.
33. European Commission. Regulation (EC) No. 1907/2006 of the European Parliament and of the Council of 18 Dec. 2006 concerning the registration, evaluation, authorisation and restriction of chemicals (REACH), establishing a European Chemicals Agency, amending directive 1999/45/EC and repealing Council Regulation (EC) No. 1488/94 as well as Council Directive 76/769/EEC and commission directives 91/155/EEC, 93/67/EEC, 93/105/EC and 2000/21/EC. *Off. J. Eur. Union, L 396/1 of 30.12.2006*; Office for Official Publication of the European Communities (OPOCE): Luxembourg, 2006.
34. OECD, Report on the regulatory uses and applications in OECD member countries of (quantitative) structure-activity relationship [(Q)SAR] models in the assessment of new and existing chemicals. Organization of Economic Cooperation and Development: Paris, France, 2006; Available online: <http://www.oecd.org/>, accessed January 2009.
35. OECD, Guidance document on the validation of (quantitative) structure-activity relationship [(Q)SAR] models. OECD series on testing and assessment No. 69. ENV/JM/MONO (2007) 2. Organization for Economic Cooperation and Development: Paris, France, 2007; Available online: <http://www.oecd.org/>, accessed January 2009.
36. A.P. Worth, A. Bassan, A. Gallegos Saliner, T. I. Netzeva, G. Patlewicz, M. Pavan, I. Tsakovska, M. Vracko, The characterization of quantitative structure-activity relationships: Preliminary guidance. European Commission - Joint Research Centre: Ispra, Italy, 2005; Available online: <http://ecb.jrc.it/qsar/publications/>, accessed January 2009.
37. A.P. Worth, A. Bassan, E. Fabjan, A. Gallegos Saliner, T. I. Netzeva, G. Patlewicz, M. Pavan, I. Tsakovska, The characterization of quantitative structure-activity relationships: Preliminary

- guidance. European Commission - Joint Research Centre: Ispra, Italy, 2005; Available online: <http://ecb.jrc.it/qsar/publications/>, accessed January 2009.
38. R. Benigni, C. Bossa, T. I. Netzeva, A. P. Worth, Collection and evaluation of [(Q)SAR] models for mutagenicity and carcinogenicity. European Commission - Joint Research Centre: Ispra, Italy, 2007; Available online: <http://ecb.jrc.it/qsar/publications/>, accessed January 2009.
39. V. H. Zhao, M. T. D. Cronin, J. C. Dearden, *Quant. Struct.-Act. Relat.* 17 (1998) 131-138.
40. M. V. Putz, A. Putz, M. Lazea, L. Ienciu, A. Chiriac, *Int. J. Mol. Sci.* 10 (2009) 1193-1214.
41. J. Zhang, G. Qiao, S. Hua, Y. Yana, Z. Rena and L. Yua, *Corros. Sci.*, 53 (2011) 147-152.
42. J.R. Mohallem, T.O. Coura, L.G. Diniz, G. Castro, D. Assafrão and T. Heine, *J. Phys. Chem. A* 112 (2008), pp. 8896–8901.
43. J.A. Ciezak and S.F. Trevino, *J. Phys. Chem. A* 110 (2006), pp. 5149–5155.
44. J. Zhang, G. Qiao, S. Hua, Y. Yana, Z. Rena and L. Yua, *Corros. Sci.*, 53 (2011) 147-152.
45. M.W. Wong, M.J. Rish and K.B. Wieberg, *J. Am. Chem. Soc.* 113 (1991) 4776-4782.
46. Materials Studio Accelrys, 2009 Manual
47. Z. Szklarska-Smialowska and M. Kaminski, *Corros. Sci.*, 13 (1973) 1-10.
48. R. A. Hoffman and S. Gronowitz, *Arkiv. Kemi* 15 (1959)45.
49. L. P. Hammett, *Chem. Rev.* 17 (1935) 125-138.
50. H. H. Jaffe, *Chem. Rev.* 53 (1953) 191-261.
51. S. Gronowitz and R. A. Hoffman, *Arkiv Kemi* 16, 539 (1960).
52. K.F.Khaled, *Corros. Sci.* (In press 2011) doi:10.1016/j.corsci.2011.01.035